Applications of Time-Resolved Step-Scan and Rapid-Scan FT-IR Spectroscopy: Dynamics from Ten Seconds to Ten Nanoseconds

T. J. JOHNSON,* A. SIMON, J. M. WEIL, and G. W. HARRIS

Bruker Instruments Incorporated, 15 Fortune Drive, Billerica, Massachusetts 01821, U.S.A. (T.J.J.); Bruker Analytische Meßtechnik, Wikingerstrasse 13, 76189-Karlsruhe, Germany (A.S., J.M.W.); and Max Planck Institute for Atmospheric Chemistry, Saarstrasse 23, 55122-Mainz, Germany (G.W.H.)

The step-scan technique in Fourier transform infrared (FT-IR) spectroscopy is employed in new applications of time resolved spectroscopy (TRS). Results are demonstrated on time-resolved laser emissions and photolytically generated chemical reactions using both emission and absorption modes. New achievements in FT-IR temporal resolution are demonstrated, as well as the complementary nature of step-scan and rapid-scan time-resolved spectroscopy.

Index Headings: **Step-scan; Time-resolved spectroscopy; Fourier transform infrared.**

INTRODUCTION

There are a multitude of spectroscopic methods for studying the kinetics of dynamic phenomena. Because the frequency of light is fast relative to chemical and physical phenomena, most spectroscopic techniques are limited in principle only by the ability of the light detector and analysis system to distinguish the changes in spectral intensity with sufficient temporal and amplitude resolution. Of the many techniques used for such analyses, all have certain advantages and disadvantages.

Dynamic UV/visible absorption spectroscopy has been the most widely used, particularly since the introduction of high-power lasers. The brightness of the sources and the performance of the detectors in this region lead to great sensitivity. However, laser fluorescence experiments suffer from difficulties in quantitation, and dynamic techniques such as molecular modulation that are based on absorption suffer from lack of specificity because the absorption/emission bands are typically broad and overlapping.[1,2] Monitoring in the infrared offers distinct advantages because a series of bands is often uniquely characteristic of a given molecule (fingerprinting). However, infrared detectors have much higher noise equivalent powers (NEPs) than UV/visible detectors, and sensitivity is thus limited. Using tunable diode lasers (TDLs) in the IR improves the detection limits since they have high brightness in comparison to thermal sources and can be modulated at high (up to GHz) frequencies.[3,4] Unfortunately, TDLs tend to be less reliable than thermal sources, and the tuning range is quite limited for a given laser. Other techniques use broad-band infrared analysis including up-converting techniques such as time-resolved infrared spectral photography[5] (TRISP). This technique has both high sensitivity and speed, but is quite expensive and cumbersome for practical analysis. Ultrafast infrared spectroscopy using pump-probe techniques stems from its UV-Vis analogue in which ultrafast lasers are used to generate short pulses, the time resolution being achieved by the temporal (i.e., physical) separation of the pump and probe photons. The temporal resolution is remarkable, but both sensitivity and bandwidth are limited in the (expensive) multiple laser experiment.[6]

Very fast time-resolved studies using Fourier transform Infrared (FT-IR) have until recently been quite limited.[7,8] FT-IR is known for its throughput and multiplex advantages in comparison to dispersive spectroscopies. Until recently, though, FT-IR could provide only minimal (~1–10 Hz) temporal resolution because a complete spectrum is obtained only at the completion of one mirror scan, and the physical mass of the mirror limits this scan rate to ~50 Hz (at 8 cm^{-1} resolution) even in the fastest of interferometers. Moreover, each spectrum is not acquired instantaneously, so the scan rates need to be fast relative to the time constant of the phenomenon. With the advent of step-scan FT-IR, however, new dimensions in time-resolved FT-IR are possible because the time resolution is not achieved via the scan rate. The principles of step-scan TRS have already been described.[9–11] Briefly, in step-scan TRS the moving mirror in the spectrometer is moved in discrete steps rather than in a continuous fashion. The technique can be used for time-resolved spectroscopy of repeatable phenomena by moving the interferometer mirror to a fixed position (HeNe fringe), triggering the phenomenon, and recording the temporal evolution of the light signal at that position. The mirror is "stepped" to the next position, and the procedure repeated. At the end of the experiment, the data are transposed into interferograms corresponding to different times after trigger, and subsequently Fourier transformed to yield time-resolved spectra.[10,11] The time resolution that can be achieved is limited only by the response speed of the detector and acquisition electronics, as well as by the detector sensitivity.

Despite the fact that modern step-scan instruments have existed for more than five years, only a few applications of the time-resolved technique have been reported. Simple demonstrative experiments of flash-lamp emissions first showed the potential of the methodology.[9,10] Since that time, Hartland *et al.* have done leading work with the technique, obtaining time-resolved state-to-state emission results on radicals such as CH_2 by mon-

Received 26 March 1993.

* Author to whom correspondence should be sent.

0003-7028/93/4709-1376$2.00/0

itoring the emissions in the visible range, where photomultipler tubes provide higher sensitivity.[11-13] Heard and Hancock and co-workers have demonstrated chemiluminescence step-scan FT-IR on systems such as O + CF_2 the mid-infrared,[14-16] where the photoluminescence is ,sed to monitor the decay from highly excited rotational and vibrational states. Both these experiments have the advantage that, being emission, they are zero-background experiments. The only absorption applications reported to date are the pioneering step-scan laser photolysis studies of the bacteriorhodopsin system by Siebert and co-workers.[17] Here an intricate system was used to obtain absolute optical density changes by using a split pre-amplifier/recorder combination, a dc component for monitoring absolute light intensities, and an ac-coupled part to monitor the fast transients at a given mirror position.

However, a very wide variety of experiments using (step-scan) FT-IR for time-resolved spectroscopy can be undertaken. Because the temporal resolution depends only on the speed of the detector and acquisition electrons, very fast processes can be monitored both in absorption and in emission. Rather than present a detailed study or extended theoretical treatment of one system, it is the goal of the present work to present new results from a handful of step-scan TRS experiments. Such experiments are intended to demonstrate the advantages of step-scan FT-IR/TRS for the practicing spectroscopist interested in time-resolved infrared applications. Thereby we wish to illustrate the complementary nature of step-scan and rapid-scan TRS, as well as demonstrate ,ew achievements in FT-IR temporal resolution. Speed ıd sensitivity considerations for future applications will also be discussed.

STEP-SCAN AND RAPID-SCAN TRS: GENERAL EXPERIMENTAL

The results reported here were all obtained with the use of one of the Bruker IFS 66, IFS 66v, or IFS 88 spectrometers. All have the same interferometer; the IFS 66v is a vacuum instrument capable of operating at pressures of less than 5 mbar. The interferometer is an air-bearing voice-coil with 0.25 cm^{-1} resolution standard and 0.10 cm^{-1} (apodized) resolution as an option; with the appropriate choice of beamsplitters, detectors, etc., (TRS) measurements are possible from the far-infrared (5 cm^{-1}) to the ultraviolet (40,000 cm^{-1}). All instrumental features including source and detector switching are under software control, as well as switching between the rapid-scan and step-scan acquisition mode. Undersampling is possible at any integral multiple of the Nyquist frequency, again in both rapid- and step-scan data acquisition modes. Certain features have been incorporated into the spectrometer to enhance the step-scan TRS experiment: To improve the signal-to-noise (S/N) ratio, in-step averaging allows the experiment to be repeated any number of times at a fixed mirror position. It has also been shown[11,18] that fluctuations in trigger intensity (i.e., +he variation in the excitation laser pulse power) trans-.te directly into random noise in spectral space. For the ıast transient recorder experiments, a dual-channel hardware/software feature has been implemented to normalize the temporal evolution at a fixed mirror position proportional to the intensity of the excitation pulse. For the TRS experiments, either the 16-bit 200-kHz ADC of the spectrometer can be used, or an 8-bit nanosecond transient recorder board (TRB) is inserted into the host 486 PC. In both cases all features are software controlled, and for triggering the host PC (or TRB) can either act as the internal clock (master mode) or be triggered (TTL pulse) externally (slave mode).

TIME-RESOLVED DIODE LASER EMISSION TO 50 NANOSECONDS

Experimental Details. The mode characteristics of a diode laser emission are important to the spectroscopist.[19,20] The monochromaticity is most important for resolved rotational-vibrational work, but is also important in telecommunications since the wavelength of the transmitter must be matched to the absorption and dispersion characteristics of the optical fiber. The goal of this experiment is to examine the emission wavelengths and characteristics as the diode is pulsed, i.e., to investigate how the optical characteristics change between time zero and full emission.

Figure 1 presents a block diagram of the experiment; the pulse generator triggers the laser diode (Sharp electronics) at a frequency of ~3 kHz with an approximately 40% duty cycle. The full current amplitude (typically 40 mA) is above the threshold but below the maximum current for the diode in forward bias. Optical filters were used, allowing an undersampling of 32 (bandwidth = 493 cm^{-1}). As the diode is pulsed, a TTL signal triggers the 40-MHz transient recorder board to monitor the temporal change at a given mirror position. The beamsplitter used here was a near-infrared silicon on quartz, the detector a dc-coupled room-temperature silicon diode. Four in-step averages were taken to improve the S/N. At the conclusion of the experiment, the data were transposed from temporal intensity changes at a given mirror position to intensities at mirror positions (i.e., interferograms) for sequential times after trigger. The data were then transferred to the acquisition processor (AQP), sorted into time-sliced interferograms, and successively Fourier transformed into a series of spectra.

Results. Figure 2 displays typical results from such a GaAs diode laser emission. The time between successive slices is 50 ns, and the spectral resolution 0.50 cm^{-1}. This resolution is more than sufficient to resolve between two modes but obviously lower than the individual linewidth of any given longitudinal mode of the diode cavity (typically <50 MHz). As seen in the figure, the diode reaches threshold at ~10 × 50 ns = 500 ns, but the natural impedance of the pulse generator and the diode results in the emission reaching a steady state after approximately (80 × 50 ns =) 4000 ns. At shorter times (i.e., before the current pulse maximizes) the emission is nearly monomode at 12,584 cm^{-1}. As the pulse generator nears full current, a second mode (to the red) rapidly grows in, obtaining nearly the intensity of the first mode after ~3500 ns. Although the bias current was kept below the maximal recommended value, it was also observed that long-term operation slowly led to multimode behavior, the new modes appearing on the red side.

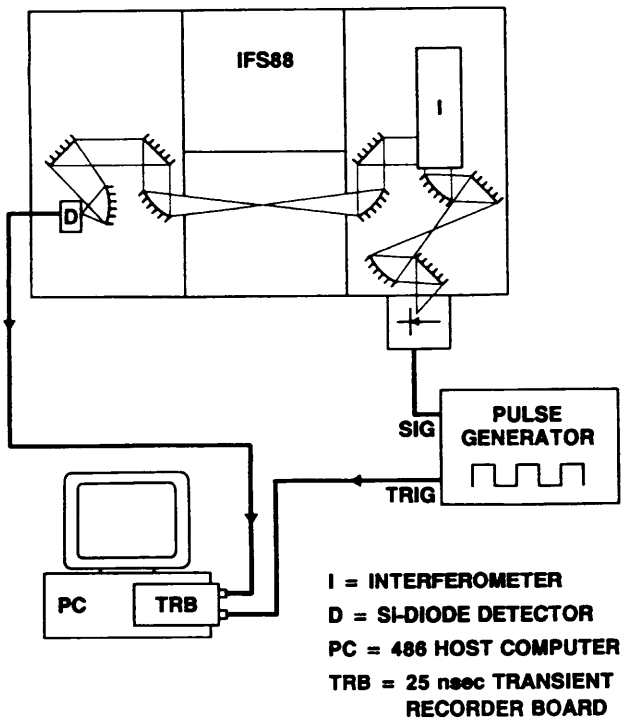

FIG. 1. Experimental outline of step-scan time-resolved diode laser emission. IFS 88 spectrometer; GaAs diode source; Si/quartz beamsplitter; Si-diode detector (dc-coupled).

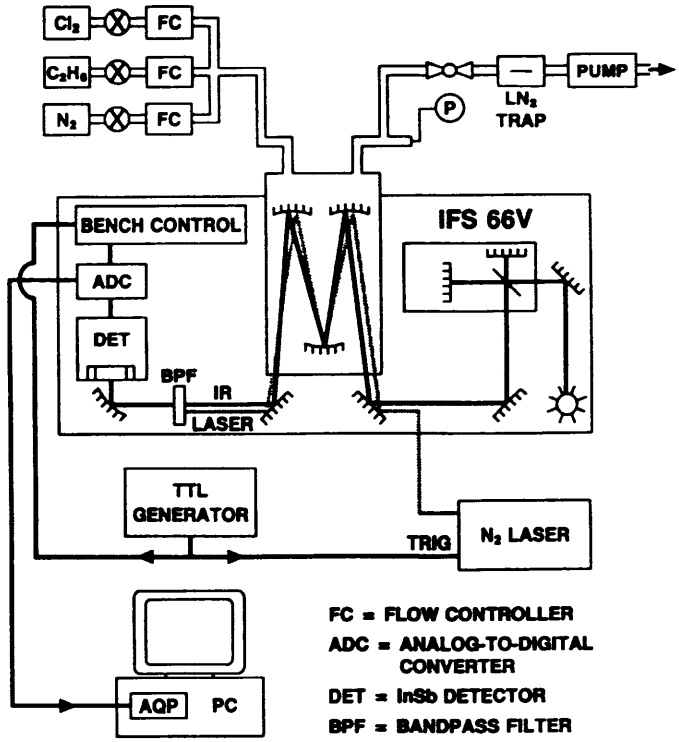

FIG. 3. Experimental schematic of step-scan time-resolved gas-phase photolysis absorption of $Cl_2/C_2H_6/N_2$ system. IFS 66v spectrometer; glowbar source; CaF_2 beamsplitter; InSb detector. N_2-laser wavelength: 337 nm.

GAS-PHASE PHOTOCHEMICAL KINETICS TO 5 MICROSECONDS

Experimental Details. One of the greatest potentials for step-scan FT-IR/TRS lies in the area of monitoring reactant and product species, as well as transient intermediates, in physical and chemical kinetics. One of the goals of the present step-scan work is to undertake some of the first absorption experiments whereby the well-known throughput and multiplex advantages of FT-IR can be coupled with fast time resolution. (Leone and coworkers have also done microsecond time-resolved FT-IR, but the temporal resolution was obtained in a more complicated inter-leaved rapid-scan manner.[7,8]) Towards this goal we chose to investigate the gas-phase photolysis of chlorine to atoms which in turn abstract a hydrogen from ethane to form HCl:

$$Cl_2 + h\nu \rightarrow 2\,Cl\cdot \quad (1)$$

$$Cl\cdot + C_2H_6 \rightarrow HCl + C_2H_5\cdot \quad (2)$$

$$Cl_2 + C_2H_5\cdot \rightarrow Cl\cdot + C_2H_5Cl. \quad (3)$$

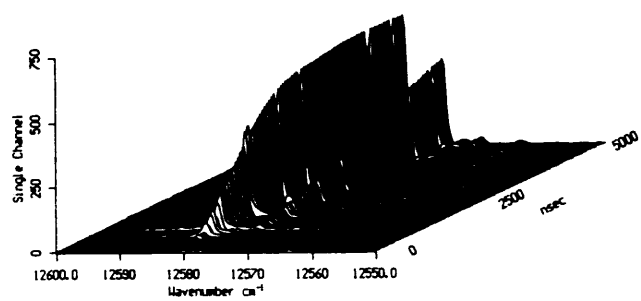

FIG. 2. Time-resolved spectra of the emission of a GaAs diode laser. Spectral resolution = 0.40 cm^{-1}, temporal resolution = 50 ns.

The reactions can continue with further H-atom abstraction from the C_2H_5Cl product, and can be terminated by several different radical recombinations.[5]

The photolysis was initiated by a (relatively weak) 200-μJ N_2 laser (Laser Science) pulsing at 337 nm (Fig. 3). Partial pressures in the reaction cell were adjusted with the use of the relative flow rates of the flow controllers (Tylan). The gas (Messer-Griesheim) partial pressures used were in the ratio 3.3:1:200 (Cl_2:C_2H_6:N_2) with a throttle valve before the pump regulating the total pressure to 33 mbar. The photolysis laser beam was sent colinearly with the infrared beam into a multiple-pass White Cell adjusted for 5.4-m total pathlength. The IFS 66v was used with a glowbar source and a CaF_2 beamsplitter. A dielectric bandpass filter after the gas cell rejected the laser line and narrowed the IR bandwidth to 2500–3300 cm^{-1}. The detector was a dc-coupled InSb photovoltaic type. Because this detector had a rise time of ~4 μs, the 16-bit, 200-kHz internal ADC was used. Although somewhat slower than other acquisition setups, the dc-coupled detector plus 16-bit ADC can be used to allow the full dynamic range of the single-beam spectrum to be incorporated into the signal. That is to say, the detector's dc coupling plus the 16-bit resolution of the ADC allows an absolute intensity to be registered at each mirror position (e.g., at time $t = 0$), and thus one can obtain absolute optical densities for each time slice without having to dc–ac switch the pre-amp at each step position.[17]

In this experiment the laser flashed continuously at 10 Hz with the data acquisition slaved to the laser trigger; after the settling time at each mirror position, the spectrometer controller waits for the next laser TTL pulse

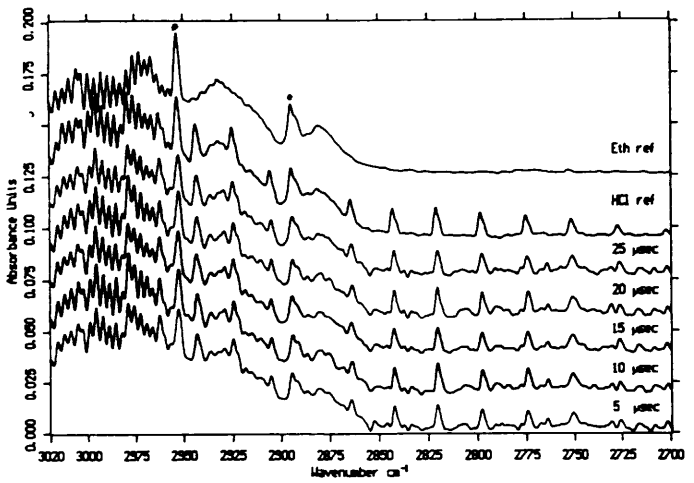

FIG. 4. Rapid-scan and step-scan time-resolved spectra of $Cl_2/C_2H_6/N_2$ system, resolution 1.6 cm^{-1}. Uppermost spectrum: absorption spectrum in rapid scan mode of photolysis mixture with photolysis laser off. Second from top: absorption spectrum in rapid-scan mode with photolysis laser running at ~25 Hz asynchronous to scan. Lower five spectra: TRS step-scan spectra corresponding to 5, 10, 15, 20, and 25 μs after the laser flash, respectively, from the bottom, with the laser running freely at 10 Hz.

to start sampling at 5-μs intervals. I_0 spectra were recorded either as step-scan spectra of the N_2-purged or empty cell or by the use of averaged rapid-scan spectra scaled to match the overall intensity of the step-scan single-beam profile. For C_2H_6 and HCl line reference positions, we recorded rapid-scan spectra (50 scans) while ›shing the laser asynchronously at maximum (~25 Hz) petition rates in order to generate as much HCl as possible.

Results. To resolve the HCl lines in both the HCl/C_2H_6 comparison spectra and in the step-scan TRS spectra, we set the (apodized) resolution to 1.6 cm^{-1}. The resultant spectra are presented in Fig. 4. The uppermost spectrum is the gas reaction mixture (Cl_2, C_2H_6, N_2) in rapid scan with the photolysis laser turned off; the spectrum below it is the asynchronous HCl photolysis rapid-scan reference; and the lowest five spectra are step-scan TR spectra corresponding to 5, 10, 15, 20, and 25 μs after the laser flash, respectively, each step-scan spectrum representing an average of 9 scans. The closely spaced lines in the 2950–3020 cm^{-1} region as well as the two strong lines marked with an asterisk (*) are ethane reactant,[5] as is the broad underlying structure near 3000 cm^{-1}. The individual lines between 2700 and 2880 are the HCl *P*-branch lines, and some of the *R*-branch lines are discernible amid the C_2H_6 absorptions at higher wavenumbers. The spectra clearly show the photolytically generated HCl already being detected within 5 μs. The successive spectra show, however, little variation in the HCl concentration. Apparently either the H-abstraction was faster than the temporal detection limit or residual HCl remained in the cell; i.e., the pumping speed was insufficient. HCl is known to exhibit long memory effects in long-path gas cells.[21] We point out that the ordinate ›r the (unshifted) lower spectra is absolute; the strong-›t HCl lines (e.g., the $J = 2 \leftarrow 3$ line at 2821 cm^{-1}) correspond to an absorbance of ~1.3×10^{-2} with a peak-to-peak S/N of ~5:1, indicating a detection limit of < ~3 $\times 10^{-3}$ OD, in spite of the low transmission of the long-path cell. We also point out that the noise was stochastic between different spectra in that continued averaging improved the signal-to-noise ratio, and in principle would have improved it further.

The observed time dependance of the product HCl in this experiment did not obey the exponential growth curve predicted by the kinetic equations. Further investigation (see below) demonstrated that this response was because of limitations in the gas exchange times in the long-path cell set by the available gas-handling equipment. It would have been desirable to increase the amount of HCl produced per pulse, but even at the lowest Cl_2 mixing ratios employed in this study the full (200 μW) output of the N_2 laser was absorbed in the long-path cell, fundamentally limiting HCl production. With more powerful lasers, and if necessary with more extended signal averaging, it is clear that many possibilities exist for detecting products and intermediates in the microsecond time domain in *absorption* mode. In an assessment similar to that of Siebert and co-workers,[17] we estimate that, after we take into account laser jitter (pulse-to-pulse stability), detector noise, etc., realistic detection limits of ~10^{-4} OD with the use of such techniques are possible.

RAPID-SCAN GAS-PHASE ABSORPTION TO 200 MILLISECONDS

Experimental. In light of the above experiment, we wanted to determine the effective residence time for HCl in the long-path gas cell under the given experimental conditions. This approach highlights an advantage of a step-scan/rapid-scan system, namely, the ability to cover different time domains with minimal hardware change; at low resolution the interferometer is capable of >80 interferograms/second in rapid-scan mode. The experimental configuration is nearly the same as that of Fig. 3, only now the controller sends out the pulse to trigger the photolysis laser. The software's internal clock is simultaneously reset to time zero and the interferometer scanned at a high rate, the successive scans being written to buffer, each scan corresponding to a certain time window after trigger. The controller then flashes the laser again, and the sequence is repeated to signal average in scan; the entire sequence corresponds to a ~2.5-s measurement cycle. Because the resolution was increased to 1.0 cm^{-1} (larger mirror travel) and because the cell exchange time was assumed to be relatively slow, the mirror scan rate was set to ~5 Hz. Since we wanted to monitor the HCl exchange time, the spectrum was monitored primarily in the *P*-branch region between 2700 and 2900 cm^{-1}.

Results. Figure 5 presents a time-slice stacked plot result of the rapid-scan photolysis experiment. The scan rate was ~5 Hz (~0.2 s/spectrum), and each slice corresponds to an actual acquisition time of 0.103 s. For plotting, we further interpolated one time between each two spectra so that the time spacing between the displayed slices is 0.092 s. The final time slice thus corresponds to ~1.8 s after the N_2-laser flash.

Observation shows that the higher resolution (1.0 rather than 1.6 cm^{-1}) is sufficient to resolve the HCl^{35}/HCl^{37} isotope lines without sacrificing significant temporal res-

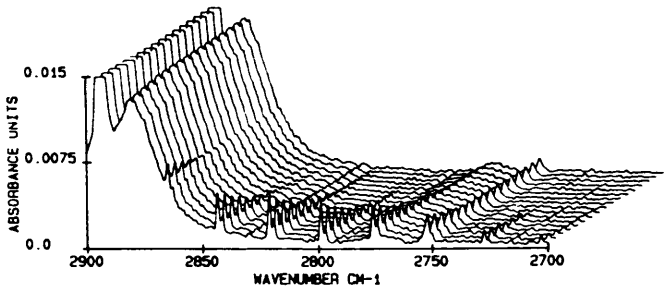

FIG. 5. Time-resolved rapid-scan spectra of $Cl_2/C_2H_6/N_2$ system on the IFS 66v spectrometer. Spectral resolution 1.0 cm^{-1}; temporal resolution = 0.092 s between slices. See text for discussion.

olution. By following one of the stronger HCl lines, we can see that the half-life for cell exchange rate at these concentrations and 33 mbar total pressure is ~0.5 s. Only at times ≥1.5 s after the laser flash is the HCl removed to below the detection limits. This pattern explains why, in the previous experiment (where the laser was pulsed at 10 Hz), one sees an effectively steady-state concentration of HCl. A small persistent feature near 2752 cm^{-1} is presumably due to trace impurities in the N_2/Cl_2 bottle. It is also worth noting that the ordinate is absolute, and that on extrapolating back to $t = 0$, we find that the absorbance of HCl generated immediately after the flash is OD ≃ 0.0037. This result is consistent with the step-scan experiment instantaneously measured HCl OD of ~0.013 when one accounts for the 10-Hz laser flash rate and the cell exchange time.

Nd:YLiF LASER EMISSION TO 10 NANOSECONDS

Experimental. Very recent improvements in transient recorder technology have now enabled 200-MHz acquisition rates at 8-bit precision. We have recently implemented such a board and, as a test analogous to that presented above, we investigated the temporal emission characteristics of a laser. In this case, a Q-switched diode-pumped Nd:YLiF [Adlas DPY 321Q (YLiF)] laser emitting at 1.047 μm (9550 cm^{-1}) was used, and the spectral acquisition rate was 10 ns. An external trigger generated by the acquisition board switches on the pumping laser diode, and the individual modes of the diode change over time. After some nanoseconds, the Q-switch is activated and the laser line at 1.047 μm appears. More specifically, Fig. 6 shows how, after the mirror stabilizes on a laser zero-crossing, the transient recorder board clock sends a signal to the pulse generator which triggers the diode laser emission. Because the laser is bright and the detector sensitive at these wavelengths, the light level was reduced by focusing the emitted light through a 1.064-μm holographic notch filter normally used for FT-Raman experiments; this step reduced the emitted intensity by at least two orders of magnitude before the interferometer.

The GaAs pumping diode emission and subsequent Nd:YLiF pulse are recorded at each mirror step by a Si diode detector. The transient signal is taken directly from the detector to the fast recorder board, with the internal clock of the board used to control the timing. As usual, the host PC records the data, and sequentially

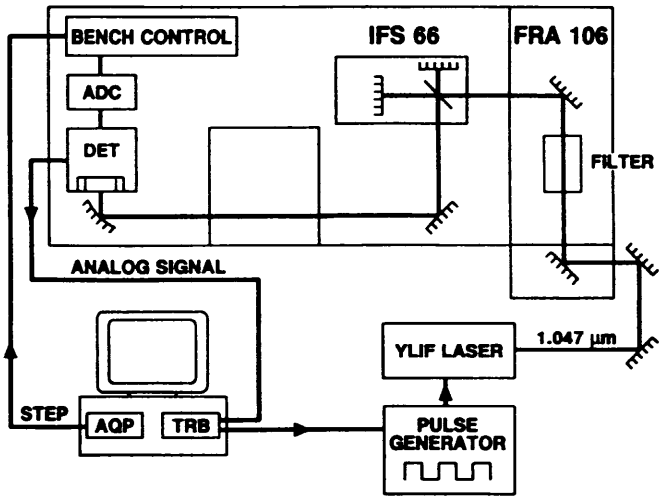

FIG. 6. Experimental schematic of step-scan 1.047-μm (9550 cm^{-1}) time-resolved emission of Q-switched Nd:YLiF laser emission. IFS 66 spectrometer; quartz beamsplitter; Si-diode detector. The filter is a 1.064-μm notch filter normally used for FT-Raman; here it reduced the laser intensity by at least two orders of magnitude.

transfers them to the AQP, which sorts them and Fourier transforms the individual interferograms into spectra.

Results. As the multimode GaAs laser emits, it pumps the Nd:YLiF laser, achieving the population inversion in the medium. The opto-electronic switch then changes the Q of the resonator so that the stimulated emission is triggered from the upper level. The resulting emissions are presented in Fig. 7. For plotting purposes, the two spectral regions of interest were concatenated on the same plot. The time scale for both is constant at 10 ns per slice. For the first ~500 ns (50 × 10 ns) after the pulse the GaAs laser is emitting and pumping the crystal. At approximately 800 ns the Q-switch is activated, and the stimulated emission of the crystal is recorded.

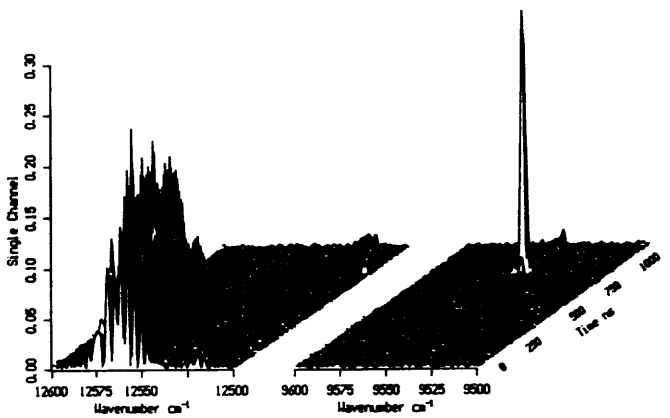

FIG. 7. Time-resolved step-scan emission spectra of emission of Q-switched Nd:YLiF laser. Spectral resolution 2 cm^{-1}; temporal resolution 10 ns. The spectra on the left show the emission of the pumping diode, and those on the right (same time scale) record the emission of the Nd:YLiF crystal.

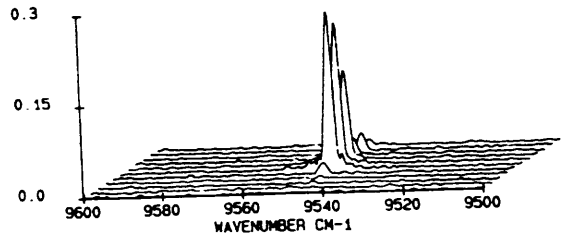

FIG. 8. Expanded (along time axis) plot of the Nd:YLiF emission of Fig. 7. Spectral resolution 2 cm^{-1}; temporal resolution 10 ns.

For pulsed sources such as Q-switched lasers, it is not only the laser wavelength but also the jitter (i.e., pulse-to-pulse intensity stability as well as the time duration and variation of the pulse after trigger) that is of importance. One of the possibilities that nanosecond step-scan FT-IR opens up is the possibility of recording the rise and fall time of such a laser pulse, while still retaining the spectral information, i.e., the exact wavelength of the pulse. This particular laser is quoted as having a 17-ns rise time for the pulse.[22] One can see from the figure that the 9550-cm^{-1} emission is switched on after ~800 ns, and the expanded plot (Fig. 8) shows that indeed the rise and decay times are both on the order of 15 ns. There is also a slight residual emission at 9550 cm^{-1}, presumably due to the continued pumping of the crystal by the diode, i.e., spontaneous rather than stimulated emission.

SUMMARY AND DISCUSSION

We have demonstrated the potential of a combined p-scan/rapid-scan spectrometer for doing time-re-ved spectroscopy. Although limited in temporal resolution, rapid-scan TRS still retains all the traditional advantages of FT-IR, namely, the throughput and multiplex advantages, as well as the use of optical and electronic filters to eliminate noise belonging to Fourier domains other than that of the measurement. In the step-scan mode, however, the fundamentally different mode of data acquisition allows TRS to be performed many orders of magnitude faster than previously possible, while still retaining Jacquinot's and Fellgett's advantages. Optical filters are possible, but electronic bandwidth considerations are different. For the rapid-scan technique, we have shown the utility at high (spectral) resolution in the absorption mode in such fields as chemical kinetics.

For the step-scan method, we have demonstrated emission experiments of lasers at high spectral resolution, as well as at temporal resolutions (10 ns) faster than any FT-IR measurements reported to date.[8,11] The ultrafast TRS also opens up the possibility of investigating nanosecond time-scale phenomena with relative ease since all the software and hardware are integrated into one complete spectrometer, with a relatively simple user interface. This capability also applies to the 5-μs absorption experiments reported here, whereby using the internal ADC and a dc-coupled detector greatly facilitates the ability to record absolute optical densities on a microsecond time scale.

The step-scan TRS method is restricted in application to events that can be repeated (reproducibly) a very large number of times. However, there are a large number of such phenomena in chemical and physical kinetics, typically triggered by a laser flash, that are highly amenable to such analysis. The combination of the step-scan technique, more and better lasers, and faster MCT and InSb detectors in the mid-infrared, as well as devices such as PMTs in the visible, along with quicker transient recorders and ADCs, shows that the technique holds great promise for doing time-resolved spectroscopy in both absorption and emission modes.

ACKNOWLEDGMENTS

We thank Dr. M. K. Welte for recording the Nd:YLiF laser emission, as well as Dr. A. Rager for assistance in preparing the manuscript. We also acknowledge the ADLAS laser company for the loan of the Q-switched Nd:YLiF laser.

1. T. T. Paukert and H. S. Johnston, J. Chem. Phys. **56**, 2824 (1972).
2. J. N. Crowley and G. K. Moortgat, J. Chem. Soc. Far. **88**, 2437 (1992).
3. T. J. Johnson, F. Wienhold, J. Burrows, and G. W. Harris, Appl. Opt. **30**, 407 (1991).
4. T. J. Johnson, F. G. Wienhold, J. P. Burrows, G. W. Harris, and H. Burkhard, "A TTFM Spectrometer for Detection of Transient Radical Species: $2\nu_1$ Overtone Absorption Lines of HO_2 at 1.5 μm," in *Monitoring of Atmospheric Pollutants with Tunable Diode Lasers*, Freiburg Symposium 1991, R. Griesar, H. Boettner, M. Tacke, and G. Restelli, Eds. (Kluwer Academic Publishers Dordrecht, 1992), pp. 183–190.
5. L. Rimai, E. W. Kaiser, E. Schwab, and E. C. Lim, Appl. Opt. **31**, 350 (1992).
6. P. O. Stoutland, R. B. Dyer, and W. H. Woodruff, Science **257**, 1913 (1992).
7. S. R. Leone, Acc. Chem. Res. **22**, 139 (1989).
8. C. M. Lovejoy, L. Goldfarb, and S. R. Leone, J. Chem. Phys. **96**, 7180 (1992) and references therein.
9. R. A. Palmer, C. J. Manning, J. A. Rzepiela, J. M. Widder, and J. L. Chou, Appl. Spectrosc. **43**, 193 (1989).
10. A. Simon and J. M. Weil, Bruker Application Note #39 (1989).
11. G. V. Hartland, W. Xie, H. L. Dai, A. Simon, and M. J. Anderson, Rev. Sci. Instr. **63**, 3261 (1992).
12. G. V. Hartland, W. Xie, D. Qin, and H. L. Dai, J. Chem. Phys. **97**, 7010 (1992).
13. G. V. Hartland, D. Qin, and H. L. Dai, J. Chem. Phys. **98**, 2469 (1993).
14. P. Biggs, G. Hancock, D. E. Heard, and R. P. Wayne, Meas. Sci. Tech. **1**, 630 (1990).
15. G. Hancock and D. E. Heard, Chem. Phys. Lett. **158**, 167 (1989).
16. G. Hancock and D. E. Heard, J. Chem. Soc. Far. **87**, 1045 (1991).
17. W. Uhmann, A. Becker, C. Taran, and F. Siebert, Appl. Spectrosc. **45**, 390 (1991).
18. S. Leone and J. Lundberg, private communication.
19. F. Slemr, G. W. Harris, D. R. Hastie, G. I. Mackay, and H. I. Schiff, J. Geophys. Res. **91**, 5371 (1986).
20. T. J. Johnson, F. G. Wienhold, J. P. Burrows, G. W. Harris, and H. Burkhard, J. Phys. Chem. **95**, 6499 (1991).
21. G. W. Harris, D. Klemp, and T. Zenker, J. Atm. Chem. **15**, 327 (1992).
22. Technical Specification Sheet for DPY 321Q pulsed Nd:YLiF laser (Adlas Laser Corporation, Luebeck Germany, 1992).